JOC The Journal of Organic Chemistry

Article

pubs.acs.org/joc

Synthetic Tripodal Receptors for Carbohydrates. Pyrrole, a Hydrogen Bonding Partner for Saccharidic Hydroxyls

Oscar Francesconi,[†] Matteo Gentili,[†] and Stefano Roelens*[,‡]

[†]Dipartimento di Chimica and [‡]Istituto di Metodologie Chimiche (IMC), Consiglio Nazionale delle Ricerche (CNR), Dipartimento di Chimica, Università di Firenze, I-50019 Sesto Fiorentino, Firenze, Italy

Supporting Information

ABSTRACT: The carbohydrate recognition properties of synthetic tripodal receptors relying on H-bonding interactions have highlighted the crucial role played by the functional groups matching saccharidic hydroxyls. Herein, pyrrole and pyridine, which emerged as two of the most effective H-bonding groups, were quantitatively compared through their isostructural substitution within the architecture of a shape-persistent bicyclic cage receptor. NMR and ITC binding studies gave for the pyrrolic receptor a 20-fold larger affinity toward octyl-β-D-glucopyranoside in $CDCl_3$, demonstrating the superior recognition properties of pyrrole under conditions in which differences would depend on the intrinsic binding ability of the two groups. The three-dimensional structures of the two glucoside complexes in solution were elucidated by combined NMR and molecular mechanics computational techniques, showing that the origin of the stability difference between the two closely similar complex structures resides in the ability of pyrrole to establish shorter/stronger H-bonds with the glucosidic ligand compared to pyridine.

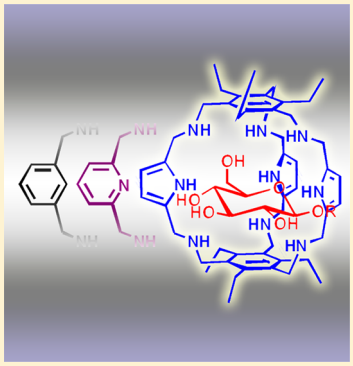

INTRODUCTION

Although molecular recognition of carbohydrates has been long recognized as a fundamental process in living organisms,[1] artificial biomimetic recognition still poses a formidable challenge in the design of synthetic receptors.[2] Indeed, structural complementarity, an essential requirement for effective recognition, must be associated with a correct choice of functional groups, in order to exploit the driving forces involved in carbohydrate recognition in biological systems. Hydrogen bonding (H-bonding) is undoubtedly a major interaction in the recognition process, which must, however, compete with water in the biological medium. Finding the most effective H-bonding groups is therefore central in the design of biomimetic receptors.

In the past few years, we have developed a family of tripodal receptors for carbohydrates based on the hexasubstituted benzene scaffold.[3] Exploiting a combination of aminic and pyrrolic H-bonding groups, we have designed and prepared a number of synthetic receptors featuring aminopyrrolic chelating arrays, which showed up to millimolar affinities for monosaccharidic glycosides in a polar organic solvent,[3c,e−i] followed by second-generation structures, in which a diaminopyrrolic H-bonding arrangement enhanced the binding ability of the receptors up to micromolar affinities.[3a,b,d]

In the course of our studies focused on this tripodal architecture, the amino/diaminopyrrolic arrangement, appropriately positioned on the binding arms of the scaffold, distilled as the most effective combination of H-bonding functions for the recognition of carbohydrates, out of a significant selection of well-established H-bonding groups, alone or in combination, including urea,[3j] amide, ester,[3h] catechol,[3g] acetal,[3f] sulfonamide, nitrone, ether, imidazole, and indole.[3c] All of these functions gave synthetic receptors endowed with poor recognition abilities, unless when in combination with pyrrole or aminopyrrolic units. On the other hand, aminic and diaminic receptors devoid of pyrrolic groups showed affinities damped by 2−3 orders of magnitude with respect to their pyrrolic counterparts,[3a,h] demonstrating the fundamental contribution to binding from the pyrrolic H-bonding group.

Thus far, from this systematic scrutiny of H-bonding functions, pyrrole emerged as the best H-bonding partner of saccharidic hydroxyl groups, subjected to the achievement of a correct binding geometry. Yet, in the past decade, a family of structurally related tripodal architectures featuring aminopyridinic binding arms has been reported by Mazik and coworkers as effective receptors for carbohydrates,[4] showing affinities for mono- and disaccharidic glycosides in organic solvents of low to medium polarity. The substantial difference characterizing the two families of architectures lies in the use of pyridinic acceptors in place of pyrrolic donors as the main H-bonding functions interacting with the hydroxylic groups of the carbohydrate.

In search for the optimal H-bonding group to improve the recognition properties of our synthetic receptors, we devised a strategic design of the receptor architecture that would allow a quantitative evaluation, all other things being equal, of the intrinsic H-bonding ability of pyrrole versus pyridine toward the carbohydrate hydroxyl groups, that is, under conditions in

Received: June 27, 2012
Published: August 10, 2012

dx.doi.org/10.1021/jo301341c | J. Org. Chem. 2012, 77, 7548−7554

Scheme 1. Chemical Structures with Atom Numbering of the Cage Compounds and of the Saccharidic Ligand (Octyl-β-D-glucopyranoside) Investigated

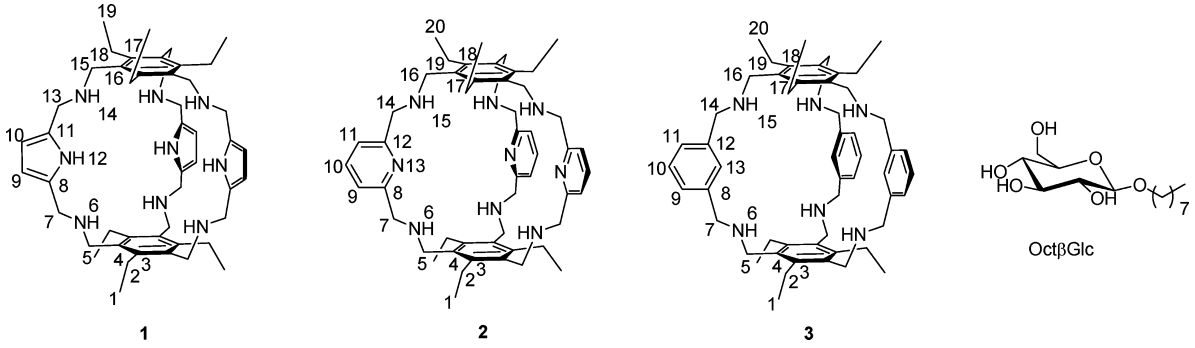

which the only difference would reside in the H-bonding ability of the pyrrolic donor versus the pyridinic acceptor.

In this article, we report quantitative evidence of the superior H-bonding properties of pyrrole when implemented in synthetic receptors fulfilling structural complementarity with the target carbohydrate, and we characterize the structural features that account for the preference for saccharidic hydroxyl groups shown with respect to pyridine.

RESULTS AND DISCUSSION

In a previous paper, we have reported that the bicyclic cage receptor **1** (Scheme 1) selectively recognizes octyl-β-D-glucopyranoside (Octβ**Glc**) with micromolar affinity in $CDCl_3$, and that the 1:1 complex is under slow-exchange regime on the NMR time scale, showing a separate set of signals for the free and the complexed species.[3i] The shape-persistent structure of **1** is ideal for the isostructural replacement of pyrrolic with pyridinic moieties, in that replacement of a H-bonding nitrogen donor with a H-bonding nitrogen acceptor would be achieved, leaving the structure of the receptor essentially unaltered. To support this hypothesis, a conformational search run on the macrobicyclic architecture gave for **1** and for its pyridinic analogue **2** (Scheme 1) closely similar minimum energy structures (Figure S1, Supporting Information).

The pyridinic cage **2**[5] was prepared following the procedure described for the synthesis of **1**,[3i] which gave the analytically pure compound in 68% yield. The benzenic analogue **3**[6] (Scheme 1), which would serve as a reference compound in binding studies featuring a H-bonding "inactive" benzene group, was also prepared through the same procedure in 71% yield. Comparison between the X-ray structure of the hexamethyl homologue of **3**[6a] and that of **1**[3i] clearly showed the close structural analogy of the two cages, proving the assumption that the replacement of benzene for pyrrole is isostructural indeed.

The binding properties of the cage receptors were evaluated through ^{1}H NMR titrations of the test glucoside. In order to obtain a homogeneous comparison of affinities, the binding abilities of **2** and **3** were tested toward Octβ**Glc** under the same conditions used for **1** ($CDCl_3$, 298 K). Selected spectra from the titrations of Octβ**Glc** with **2** and **3** are reported in Figure 1 and Figure S2 (Supporting Information), respectively. Despite the extensive overlap of signals, the formation of the slow-exchanging 1:1 complex is clearly evident in both cases, delineating a close analogy with the results obtained for **1**. However, the fraction of bound Octβ**Glc** observed for a 1:1

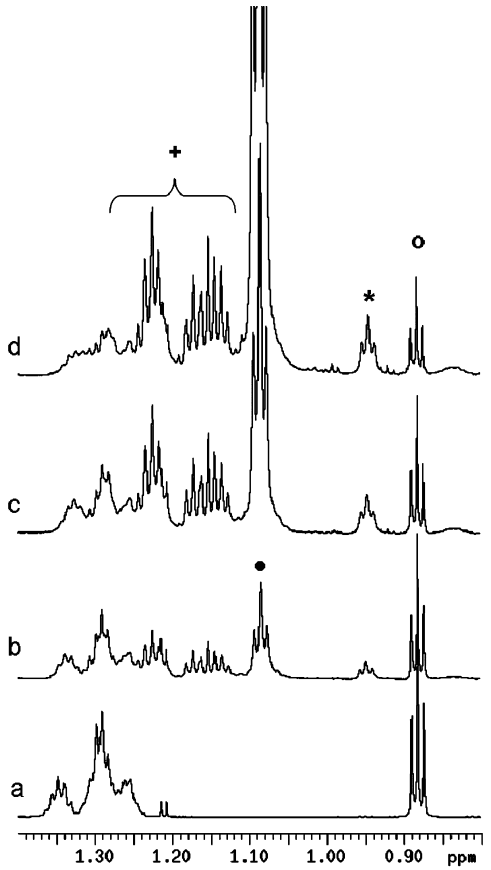

Figure 1. Selected spectral region of the ^{1}H NMR titration (900 MHz, $CDCl_3$, 298 K) of Octβ**Glc** (1.27 mM) with increasing concentration of receptor **2**: (a) 0 mM, (b) 0.580 mM, (c) 1.30 mM, (d) 2.60 mM. The signals of the free reactants [**2** (●); Octβ**Glc** (○)], and of the 1:1 complex [**2** (+); Octβ**Glc** (*)] are indicated in the figure.

mol ratio of reactants is significantly smaller than that observed with **1** in the case of **2**, and even smaller in the case of **3**, pointing to weaker binding affinities. Binding constants for the 1:1 complexes were obtained by integration of the available signals, averaged over at least three spectra, and reported in Table 1 as K_d values, together with the value previously obtained for **1**[3i] for direct comparison. It is immediately apparent that affinities of the three receptors for Octβ**Glc** differ by orders of magnitude, with K_d of **1** being over 40 times smaller than that of **2** and over 260 times smaller than that of **3**. If the binding ability of **3** is essentially due to the contribution of the aminic groups, the increase in affinity of **1** and **2**

dx.doi.org/10.1021/jo301341c | J. Org. Chem. 2012, 77, 7548−7554

Table 1. Dissociation Constants K_d[a] with Standard Deviation (σ) for 1:1 Complexes of Cage Receptors with OctβGlc

method	1	2	3
NMR[b]	20.7 ± 0.4[d]	849 ± 59	5290 ± 308
ITC[c]	25.1 ± 0.6	275 ± 6	4960 ± 60

[a]Thermodynamic equilibrium constants referred to a 1 μM standard state. [b]Measured by ^{1}H NMR (900 MHz) in $CDCl_3$ at T = 298 K. [c]Measured by ITC in $CHCl_3$ at T = 298 K. [d]See ref 3i.

quantifies the contribution of the H-bonding capability of the pyrrolic NH donor with respect to the pyridinic N acceptor. It is important to stress that this ranking is grounded on the isostructural replacement of the two groups within the well-defined geometry of the cage receptor.

A closer inspection of the spectral features revealed a significant shift of the free OctβGlc signals along the titration of **2**, not occurring in the titrations of **1** and **3**, which is evidence of fast exchange in solution between the free glucoside and complex species other than the slow-exchanging 1:1 complex (Figure S3, Supporting Information). While this does not question the formation of the 1:1 complex, it affects the measure of the equilibrium concentration of the actual free glucoside used for calculating the binding constant, which therefore results in underestimation.

In order to confirm the NMR binding data through an independent technique and to obtain a more accurate value for the affinity of **2**, calorimetric ITC titrations were performed under the same conditions ($CHCl_3$, 298 K). The results reported in Table 2 as cumulative formation constants and in Table 1 as dissociation constants for comparison with the NMR results show a gratifyingly good agreement between the K_d values for **1** and **3** obtained by the two techniques, whereas, as anticipated, the value for **2** is smaller than that obtained from the NMR titration, due to the presence of a fast-exchanging adduct affecting the equilibrium concentrations. Since only a 1:1 association could be detected by ITC titrations, the fast-exchanging species was ascribed to an "externally bound" 1:1 adduct which, together with the "caged" complex, would be detected as one thermodynamic macrospecies by ITC.

It should be noted that a 1:2 adduct was detected in the case of **1**, which, however, did not produce more than a negligible shift of the glucoside signals (and consequently a negligible concentration inaccuracy in the calculation of K_d) because of the overwhelming presence of the 1:1 complex. It must also be underlined that, although complex species of higher stoichiometry are formed for **1**, only the 1:1 complexes are relevant for comparing the H-bonding contribution from pyrrole and pyridine, as these species can be directly compared with all other things being equal. For this reason, only the dissociation constants of the 1:1 species have been taken into account. Thus, the overall binding affinity of the pyridinic receptor is more accurately ranked as more than 1 order of magnitude lower than that of its pyrrolic counterpart but nearly 20-fold larger than that of the reference benzenic cage. However, considering that the fast exchanging 1:1 complex also contributes to the overall affinity of the pyridinic receptor, the contribution from pyrrole with respect to that of pyridine, as detected from the cage complex exclusively, would be larger than the above figures.

Thermodynamic parameters for the 1:1 adducts of **1** and **2** show that, in both cases, complexation is enthalpic in origin, compensated, as expected, by adverse entropic contributions, and that the strong enthalpic difference between the two complexes is attenuated by a larger entropic loss for the pyrrolic receptor, resulting in a binding free energy difference of 6 kJ mol^{-1}. This is in agreement with a more strongly H-bonded complex for **1** with respect to **2**, at the expense of a significant rigidity increase. Lack of pyrrolic/pyridinic nitrogen atoms accounts for the significantly smaller binding free energy of the benzenic cage **3**, for which the reduced enthalpic contribution can be ascribed to the loss of H-bonding interactions.

To gain an insight into the structural reasons for the markedly different binding contributions from pyrrole and pyridine H-bonding groups, the binding modes characterizing the receptor to glucoside interaction in solution were investigated by NMR spectroscopic techniques. Addition of equimolar amounts of **1** or **2** to a solution of OctβGlc in $CDCl_3$ caused, as described, the appearance of a new set of signals for the 1:1 complex, at the expense of the intensity of the signals of the free species. A strong upfield shift was observed for the CH signals of the bound sugar, caused by the shielding effect of the aromatic cavity, whereas desymmetrization of the receptor structure upon binding to the chiral ligand gave rise to a very complex pattern of signals. Inclusion in the cavity is confirmed by the upfield shift of all of the CH protons on both faces of the pyranose ring. Spectral features and chemical shift data are reported in Figures S4 and S5 and Table S1 (Supporting Information). Unfortunately, chemical shift variations upon binding were not very informative, as the largest differences between the two receptors were observed for the H-6 and H-7 protons, which are dependent on the conformational motions of the side chains and not directly related to the orientation of the pyranose ring inside the cavity; rather, the similar chemical shift distribution suggests that docking of the glucoside into the receptor may be analogous for **1** and **2**, with differences hardly amenable to structural assignment.

A more defined structural picture can be retrieved from the NOESY experiments performed on equimolar solutions of OctβGlc and **1** or **2**. The results are reported in Figure S6 and Table S2 and schematically depicted in Figure S7. Unambiguous intermolecular NOE contacts were identified for **2** between the CH_2 moieties of the ethyl substituents of the

Table 2. Cumulative Constants (log βn) with Standard Deviations (σ) and Thermodynamic Parameters (kJ mol^{-1}) for the Formation of Complexes of the Cage Receptors with OctβGlc[a]

receptor	log β (R/G)	ΔG^0	ΔH^0	$-T\Delta S^0$
1	4.60 ± 0.01 (1:1)	−26.24 ± 0.06	−69.3 ± 0.2	43.1 ± 0.3
	7.57 ± 0.04 (1:2)	−43.2 ± 0.3	−73.7 ± 0.9	30.5 ± 1.1
2	3.56 ± 0.01 (1:1)	−20.34 ± 0.07	−51.7 ± 0.3	31.4 ± 0.4
3	2.304 ± 0.005 (1:1)	−13.15 ± 0.03	−49.4 ± 0.3	36.3 ± 0.4

[a]Measured by ITC in $CHCl_3$ at T = 298 K.

dx.doi.org/10.1021/jo301341c | J. Org. Chem. 2012, 77, 7548−7554

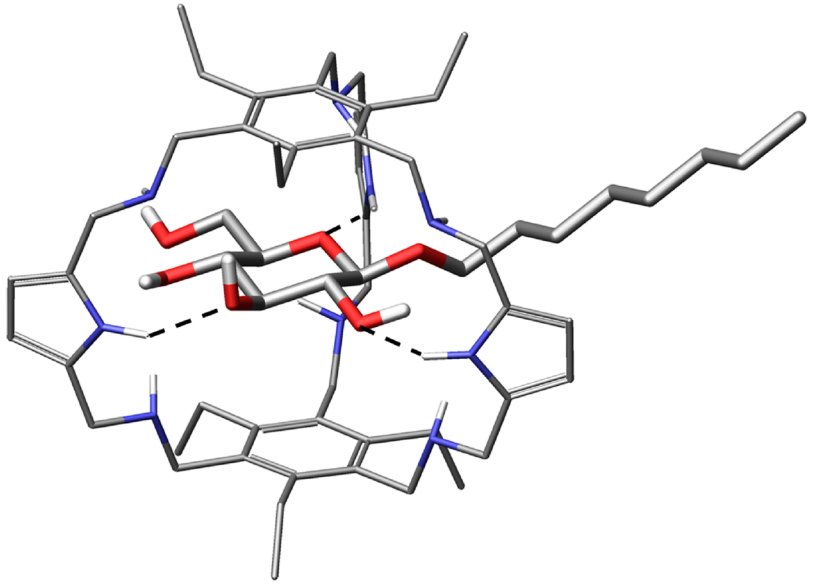

Figure 2. Global minimum structure obtained from a search of the conformational space for the complex between **1** and OctβGlc. H-bonds involving pyrrolic NH donor groups are depicted as dashed lines, and O···N interatomic distances are reported in Table 4. Selected additional distances: N−H···O-5, 1.97 Å; N−H···OH-2, 2.03 Å; N−H···OH-3, 1.97 Å.

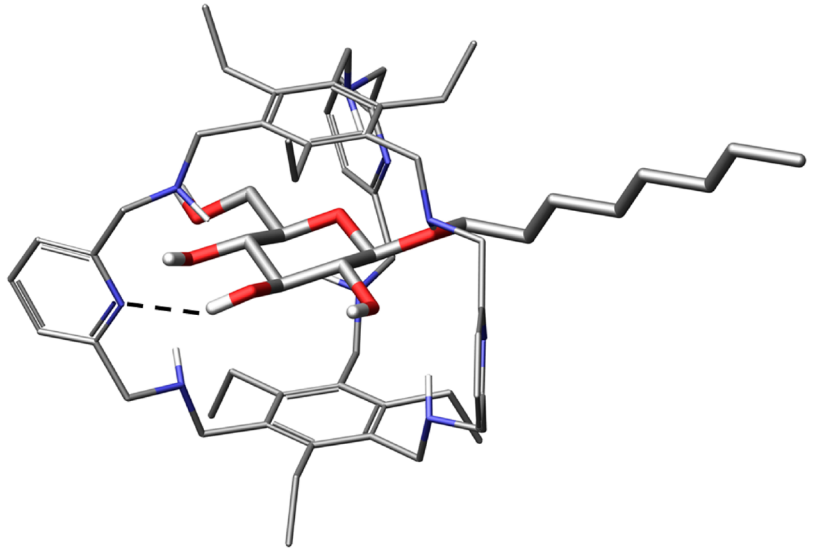

Figure 3. Global minimum structure obtained from a search of the conformational space for the complex between **2** and OctβGlc. H-bonds involving pyridinic N acceptor groups are depicted as dashed lines and O···N interatomic distances are reported in Table 4. Selected additional distances: O−H···N, 2.08 Å.

aromatic platforms and several glucoside CH protons; other intermolecular contacts were difficult to assign unambiguously because of severe signal overlap. In the case of **1**, in addition to the NOEs identified for **2**, intermolecular NOE contacts between pyrrolic and aminic NH groups and glucoside CH protons were found in a clean spectral region and unambiguously assigned. Altogether, chemical shift and NOE data demonstrated the formation of an inclusion complex of OctβGlc inside the cavity of both cage receptors; furthermore, NOE cross-peaks indicated that, for **1**, pyrrolic and aminic NH groups point toward the glucosidic guest.

Since experimental NMR data alone are not sufficient for a definition of the binding interaction modes in solution, a well-tested molecular mechanics computational protocol has been applied to model the three-dimensional structures of the complexes of OctβGlc with **1** and **2**.[7] The protocol consists of running a search of the conformational space of the complex to select the families of conformers compatible with the chemical shift and NOE experimental data. The details of the protocol are described in the Experimental Section (Supporting Information). For each of the two complexes, the conformational search of the molecular mechanics protocol gave only one family of conformers in agreement with the NMR data within 10 kJ mol^{-1} from the global minimum. In Figures 2 and 3, the global minimum structures of the two families are depicted for the OctβGlc complexes of receptors **1** and **2**, respectively, while the entire families of conformers, in which differences essentially concern the conformation of the octyl chains, are reported in Figures S8 and S9.

dx.doi.org/10.1021/jo301341c | *J. Org. Chem.* 2012, 77, 7548−7554

The observed NOE contacts, together with the corresponding distances calculated from the lowest energy conformation of the two complexes, are reported in Table 3. The good agreement that can be appreciated between experimental NOEs and calculated distances supports the view that the conformers obtained by the combined approach represent the structures that most closely describe the recognition modes adopted by receptors **1** and **2** when binding to OctβGlc.

Table 3. Observed Intermolecular NOE Contacts and Corresponding Distances (Å) Calculated from Global Minimum Structures for Complexes of OctβGlc with Receptors 1 and 2[a]

OctβGlc	1	2
H-1	NH-12 (3.16)	H-2 (3.06)
	NH-6 (3.24)	H-2′ (2.91)
	H-2 (3.12)	
H-3	NH-12* (3.15)	
H-4		H-19* (2.67)
H-5		H-2* (2.48)
H-6′	NH-12 (2.65)	H-19*′ (2.37)
	NH-6 (2.15)	
H-7	H-2 (2.38)	H-19 (2.61)
H-7′	NH-12 (1.97)	

[a]From 500 MHz NOESY spectra of a 1:1 mixture of reactants in $CDCl_3$ at T = 298 K. Asterisks denote protons become unequivalent upon complexation.

A striking similarity between the structures of the two complexes is apparent, both in terms of binding geometry and docking orientation, which further confirms that the substitution of the pyrrolic NH donor with the pyridinic N acceptor is isostructural, not only in the free receptors but also in the complexes with the glucoside. Thus, what is causing the different stabilities of the two complexes? At first glance, it can be noted that in the complex of **1** all the pyrrolic nitrogen donors are engaged in H-bonding to oxygen acceptors, including the pyranosidic oxygen, whereas in the complex of **2**, only one pyridinic nitrogen acceptor is H-bonded to the glucosidic OH-3, the other two pointing away from a bonding direction (see Figures 2 and 3 for selected distances).

Following this observation, an inventory of the possible H-bonding contacts in the two complexes was attempted by collecting in Table 4 all of the O···N interatomic distances, calculated from the minimum energy structures, shorter than the sum of van der Waals radii, and selecting those distances complying with H-bonding criteria. The result of this selection is depicted in the plots of Figure 4, in which H-bonding distances involving pyrrolic and pyridinic nitrogens (black) are distinguished from other H-bonding distances (gray) and from those distances lacking acceptable H-bonding directionality (white).

Table 4. O···N Interatomic Distances (Å) Calculated from Minimum Energy Structures for Complexes of OctβGlc with Receptors 1 and 2[a]

OctβGlc	1	2
O-5	NH-12 (2.83)	NH-15 (2.85)
	NH-14 (2.95)	
OH-2	NH-12* (2.77)	N-13* (3.02)
	NH-6* (3.02)	NH-6* (2.87)
	NH-14* (3.07)	NH-15* (3.05)
OH-3	NH-12** (2.82)	N-13** (2.97)
	NH-14** (2.90)	NH-15** (2.94)
OH-4	NH-12** (2.89)	N-13** (2.90)
	NH-6** (2.94)	NH-6** (2.90)

[a]Distances shorter than the sum of the van der Waals radii are reported. Asterisks indicate protons become unequivalent upon complexation.

It can be easily seen that the most relevant difference characterizing the two complexes is that all pyrrolic nitrogen donors are involved in H-bonding, whereas only one pyridinic nitrogen acceptor is H-bonded; furthermore, all three pyrrolic H-bonds are markedly shorter than the one established by the pyridinic nitrogen, thereby implying a stronger interaction. Considering that the H-bonding contacts established by aminic nitrogens are similar in the two complexes in terms of both number and distances,[8] it can be concluded that the origin of the larger stability of the pyrrolic cage complex lies in the abilty of pyrrolic groups to establish shorter/stronger H-bonding interactions with the sugar than pyridinic groups. Apart from the inability of pyridine to H-bond to the pyranosidic ring oxygen, the lack of interaction of the pyridinic nitrogen with OH-2 and the looser H-bond to OH-3 indicates a reduced tendency of pyridine to act as a H-bonding partner compared to the pyrrolic ring. On the other hand, the monosaccharide seems to be prone to behave as an acceptor rather than a donor of H-bonds, which favors the interaction with pyrrole with respect to pyridine. This may be ascribed to a better functional matching between the pyrrolic nitrogen and the saccharidic oxygen groups, a consideration that can be extended to the comparison with the other H-bonding groups tested so far, but it may also be related to the fact that pyrrolic donors do not need to disrupt the intramolecular H-bonding array of the glucoside[9] to establish H-bonding interactions, whereas this is necessary in the case of the pyridinic acceptor. This is indeed observed in the modeled structures of the two complexes (Figure S10, Supporting Information): two of the three intramolecular H-bonds present in the free glucoside persist in the complex of the pyrrolic receptor, whereas only one is present in the complex of the pyridinic receptor since the OH-2 to O-3 H-bond is formed when the OH-3 to O-4 H-bond is broken to bind to the pyridinic nitrogen.

CONCLUSION

In the present paper, we have shown, through NMR and ITC binding studies, that pyrrole is a superior H-bonding partner for octyl-β-D-glucopyranoside compared to pyridine when isostructurally replaced into the architecture of a shape-persistent cage receptor. Experimental NMR data and molecular mechanics calculations allowed us to model the three-dimensional structures of the complexes in solution, showing that the larger stability of the complex of the glucoside with the pyrrolic cage receptor with respect to the pyridinic counterpart lies in the ability of the former to establish shorter/stronger H-bonds while engaging all of the available pyrrolic groups. So far, pyrrole stands as a very effective H-bonding partner for the recognition of monosaccharides, among a wide variety of well-established H-bonding groups, provided that it is implemented into an architecture capable of achieving the correct binding geometry. This finding is bound to have an impact on the design of synthetic receptors for carbohydrates.

dx.doi.org/10.1021/jo301341c | J. Org. Chem. 2012, 77, 7548−7554

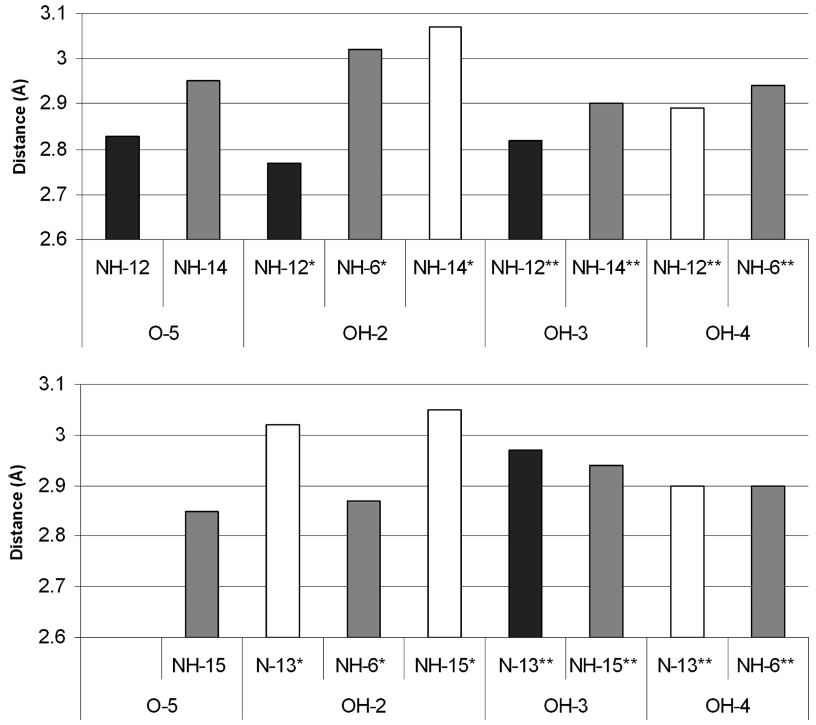

Figure 4. Plot of O···N Interatomic distances (Å) calculated from minimum energy structures for complexes of OctβGlc with receptors **1** (top) and **2** (bottom). Black: pyrrolic/pyridinic H-bonding distances. Gray: aminic H-bonding distances. White: distances lacking acceptable H-bonding directionality.

EXPERIMENTAL SECTION

NMR Methods. NMR experiments were performed on 500 and 900 MHz spectrometers at 298 K unless otherwise stated. To avoid interference of traces of acid in solution, $CDCl_3$ was treated by eluting through a short column of alumina right before use. Chemical shifts are reported in parts per million (δ) relative to TMS, using the residual solvent line as secondary internal reference (7.26 ppm for spectra run in $CDCl_3$). NMR titrations were performed in a 5 mm NMR tube calibrated at 625 μL using microsyringes. The titrant was weighed in a calibrated flask and dissolved with a stock solution of the titrate. The NMR tube was filled up to the calibrated volume with the titrant concentrated solution and subsequently diluted by stepwise addition of the titrate solution to keep the titrate concentration constant throughout. After each step, the solution in the NMR tube was syringed back to the 625 μL volume, so that titrations could be performed at a constant volume, and ^{1}H NMR spectra were acquired with high digital resolution, collecting an average of about 20 spectra for each titration. NMR binding constant measurements for receptor **1** were described in a previous paper;[3i] for receptors **2** and **3**, measurements were performed at three different receptor/glycoside mole ratios at a fixed concentration of OctβGlc, that is, from 1:1.5 to 1.5:1 for receptor **2** at 1.27 mM of glycoside and from 1:2 to 2:1 for **3** at 2.13 mM of glycoside. NMR characterization experiments on free reagents were recorded at ca. 2 mM for OctβGlc and ca. 3.5 mM for receptors **1**, **2**, and **3**, whereas for their combination, the concentrations were 1.90 and 1.98 mM for **1** and OctβGlc, respectively; 2.15 and 2.28 mM for **2** and OctβGlc, respectively; 2.32 and 2.09 mM for **3** and OctβGlc, respectively. Under these conditions, the 1:1 complex constituted the dominant species in all cases. In addition to standard 1D ^{1}H NMR spectra, COSY, TOCSY, HSQC, HMBC, and NOESY experiments were also acquired using standard sequences, in order to assign the resonances of all of the molecular entities, free and bound, as well as to detect the relevant intramolecular and intermolecular NOE contacts.

ITC Methods. Isothermal titration calorimetry experiments were performed at 298 K. After the first injection of 3 μL, the receptor solutions were stepwise injected in 12 steps of 20 μL aliquots into the sample cell containing a solution of the glucoside. An initial 1 μL dummy volume was taken into account in the concentration calculation. All experiments were performed in chloroform stabilized with amylene and filtered through a short column of basic alumina right before use. Heats of dilution were measured by injecting the receptor solution into neat chloroform and were then subtracted from the binding heats. The thermodynamic parameters and K_d values were obtained by nonlinear least-squares fitting of the experimental data using the HypCal computer program.[10]

Molecular Modeling Methods. Initial structures of OctβGlc and receptors **1**, **2**, and **3** were built using the Maestro software package.[11] All structures were minimized using conjugate gradients with the AMBER* force field[12] and a dielectric constant of 4.81 D (chloroform) with extended cutoff to treat remote interactions. A maximum number of 5000 iterations were employed with the PRCG scheme, until the convergence energy threshold was 0.05. Once the optimum geometries had been achieved, a conformational search protocol was adopted for the receptors, using a Monte Carlo torsional sampling method (MCMM) with automatic setup during the calculation, energy window of 50 kJ mol^{-1}, 1000 maximum number of steps, and 100 steps per torsion of the bond to be rotated. The best structures obtained from this calculation in terms of energy were chosen, and then, the glucoside was manually docked within the receptor cleft with different starting relative orientations and further minimized. Minimization results afford different structures which were employed as input for further conformational search protocols. Several complexes were found to be stable, in which the sugar remained inside the receptor cavity. The lowest energy structures were analyzed to check the agreement with experimental NMR data.

Materials. The octyl glucoside was purchased from commercial suppliers and used without purification. The hexamino cage receptor **1** was previously reported,[3i] and receptors **2**[5] and **3**[6] were known compounds and were prepared according to literature procedures. Materials' purity was determined by melting point range, ^{1}H NMR, ^{13}C NMR, and ESI-MS techniques.

dx.doi.org/10.1021/jo301341c | J. Org. Chem. 2012, 77, 7548−7554

■ ASSOCIATED CONTENT

Supporting Information

ITC titrations and plots; supplementary tables and figures. This material is available free of charge via the Internet at http://pubs.acs.org.

■ AUTHOR INFORMATION

Corresponding Author

*E-mail: stefano.roelens@unifi.it.

Notes

The authors declare no competing financial interest.

■ ACKNOWLEDGMENTS

High-field NMR spectra were acquired at the Magnetic Resonance Center (CERM) facilities of the Università di Firenze. We thank Mr. M. Lucci for technical assistance. Ente Cassa di Risparmio di Firenze (Italy) is acknowledged for granting an ITC nano calorimeter (Grant No. 2009.0576). A research grant to O.F. (Grant No. 2008.1475) from Ente Cassa di Risparmio di Firenze is also gratefully aknowledged.

■ REFERENCES

(1) (a) Gabius, H.-J.; André, S.; Jiménez-Barbero, J.; Romero, A.; Solís, D. *Trends Biochem. Sci.* **2011**, *36*, 298−313. (b) Gabius, H.-J., Ed. *The Sugar Code: Fundamentals of Glycosciences*; Wiley-VCH: Weinheim, Germany, 2009. (c) Murrey, H. E.; Hsieh-Wilson, L. C. *Chem. Rev.* **2008**, *108*, 1708−1731. (d) Ernst, B., Hart, W., Sinaÿ, P., Eds. *Carbohydrates in Chemistry and Biology*, Part I Vol. *2*, and Part II Vol. *4*; Wiley-VCH: Weinheim, Germany, 2000. (e) Lindhorst, T. K. *Essentials of Carbohydrate Chemistry and Biochemistry*; Wiley-VCH: Weinheim, Germany, 2000.

(2) For recent reviews, see: (a) Davis, A. P. *Nature* **2010**, *464*, 169−170. (b) Jin, S.; Cheng, Y.; Reid, S.; Li, M.; Wang, B. *Med. Res. Rev.* **2010**, *30*, 171−257. (c) Walker, D. B.; Joshi, G.; Davis, A. P. *Cell. Mol. Life Sci.* **2009**, *66*, 3177−3191. (d) Davis, A. P. *Org. Biomol. Chem.* **2009**, *7*, 3629−3638. (e) Mazik, M. *Chem. Soc. Rev.* **2009**, *38*, 935−956. (f) Kubik, S. *Angew. Chem., Int. Ed.* **2009**, *48*, 1722−1725. (g) Davis, A. P.; James, T. D. In *Functional Synthetic Receptors*; Schrader, T., Hamilton, A. D., Eds.; Wiley-VCH: Weinheim, Germany, 2005; pp 45−109.

(3) (a) Nativi, C.; Francesconi, O.; Gabrielli, G.; Vacca, A.; Roelens, S. *Chem.—Eur. J.* **2011**, *17*, 4814−4820. (b) Ardá, A.; Cañada, F. J.; Nativi, C.; Francesconi, O.; Gabrielli, G.; Ienco, A.; Jiménez-Barbero, J.; Roelens, S. *Chem.—Eur. J.* **2011**, *17*, 4821−4829. (c) Cacciarini, M.; Nativi, C.; Norcini, M.; Staderini, S.; Francesconi, O.; Roelens, S. *Org. Biomol. Chem.* **2011**, *9*, 1085−1091. (d) Ardá, A.; Venturi, C.; Nativi, C.; Francesconi, O.; Gabrielli, G.; Cañada, F. J.; Jiménez-Barbero, J.; Roelens, S. *Chem.—Eur. J.* **2010**, *16*, 414−418. (e) Ardà, A.; Venturi, C.; Nativi, C.; Francesconi, O.; Cañada, F. J.; Jiménez-Barbero, J.; Roelens, S. *Eur. J. Org. Chem.* **2010**, 64−71. (f) Nativi, C.; Cacciarini, M.; Francesconi, O.; Moneti, G.; Roelens, S. *Org. Lett.* **2007**, *9*, 4685−4688. (g) Cacciarini, M.; Cordiano, E.; Nativi, C.; Roelens, S. *J. Org. Chem.* **2007**, *72*, 3933−3936. (h) Nativi, C.; Cacciarini, M.; Francesconi, O.; Vacca, A.; Moneti, G.; Ienco, A.; Roelens, S. *J. Am. Chem. Soc.* **2007**, *129*, 4377−4385. (i) Francesconi, O.; Ienco, A.; Moneti, G.; Nativi, C.; Roelens, S. *Angew. Chem., Int. Ed.* **2006**, *45*, 6693−6696. (j) Vacca, A.; Nativi, C.; Cacciarini, M.; Pergoli, R.; Roelens, S. *J. Am. Chem. Soc.* **2004**, *126*, 16456−16465.

(4) For a comprehensive review, see: Mazik, M. *Chem. Soc. Rev.* **2009**, *38*, 935−956.

(5) (a) Mateus, P.; Delgado, R.; Brandão, P.; Félix, V. *J. Org. Chem.* **2009**, *74*, 8638−8646. (b) De Rycke, N.; Marrot, J.; Couty, F.; David, O. R. P. *Tetrahedron Lett.* **2010**, *51*, 6521−6525.

(6) (a) Arunachalam, M.; Ravikumar, I.; Ghosh, P. *J. Org. Chem.* **2008**, *73*, 9144−9147. (b) Mateus, P.; Delgado, R.; Brandão, P.; Carvalho, S.; Félix, V. *Org. Biomol. Chem.* **2009**, *7*, 4661−4673.

(7) For examples of application of NMR techniques assisted by molecular modeling, see: (a) Jiménez-Barbero, J.; Dragoni, E.; Venturi, C.; Nannucci, F.; Ardá, A.; Fontanella, M.; André, S.; Cañada, F. J.; Gabius, H.-J.; Nativi, C. *Chem.—Eur. J.* **2009**, *15*, 10423−10431. (b) Kolympadi, M.; Fontanella, M.; Venturi, C.; André, S.; Gabius, H.-J.; Jiménez-Barbero, J.; Vogel, P. *Chem.—Eur. J.* **2009**, *15*, 2861−2873. (c) Mari, S.; Cañada, F. J.; Jiménez-Barbero, J.; Bernardi, A.; Marcou, G.; Motto, I.; Velter, I.; Nicotra, F.; La Ferla, B. *Eur. J. Org. Chem.* **2006**, 2925−2933. (d) Mari, S.; Posteri, H.; Marcou, G.; Potenza, D.; Micheli, F.; Cañada, F. J.; Jiménez-Barbero, J.; Bernardi, A. *Eur. J. Org. Chem.* **2004**, 5119−5225.

(8) It must be noted, however, that amino groups differ in their donor/acceptor properties between the two complexes: in the pyrrolic complex, NH-6*···OH-2 and NH-14**···OH-3 involve aminic acceptors, while NH-14···O-5 and NH-6**···OH-4 involve aminic donors, whereas in the pyridinic complex, all of the amino groups involved in H-bonding behave as donors (see Figure 4). Due to the ambivalent H-bonding behavior of the amino group (for a crystallographic evidence, see: Hanessian, S.; Simard, M.; Roelens, S. *J. Am. Chem. Soc.* **1995**, *117*, 7630−7645), it can be misleading to consider the aminopyrrolic arrangement as a cooperative donor−acceptor pair..

(9) (a) Deshmukh, M. M.; Bartolotti, L. J.; Gadre, S. R. *J. Phys. Chem. A* **2008**, *112*, 312−321. (b) López de la Paz, M.; Ellis, G.; Pérez, M.; Perkins, J.; Jiménez-Barbero, J.; Vicent, C. *Eur. J. Org. Chem.* **2002**, 840−855.

(10) Gans, P.; Sabatini, A.; Vacca, A. *J. Solution Chem.* **2008**, *37*, 467−476.

(11) *Maestro, A Powerful, All-Purpose Molecular Modelling Environment*, version 8.5; Schrödinger, LLC, New York, NY, 2008.

(12) Case, D. A.; Cheatham, T. E., III; Darden, T.; Gohlke, H.; Luo, R.; Merz, K. M., Jr.; Onufriev, A.; Simmerling, C.; Wang, B.; Woods, R. J. *J. Comput. Chem.* **2005**, *26*, 1668−1687.